Monitoring Air/Sea Interaction Processes Using Passive Acoustic Drifters (AN/WSQ-6 Buoys)

Jeffrey A. Nystuen*
Cooperative Institute for Marine and Atmospheric Studies
Rosenstiel School for Marine and Atmospheric Sciences
University of Miami
Miami, Florida

FINAL REPORT
June 1995

Grant No: N00014-94-1-G906

Prepared for: Harry D. Selsor
Tactical Oceanography Warfare Support (TOWS) Program Office
Naval Research Laboratory - Detachment
Stennis Space Center, Mississippi

* Present address: Applied Physics Laboratory, 1013 NE 40th St., Seattle, Washington 98105

This project was sponsored by the Department of the Navy, Office of the Chief of Naval Research. The contents do not necessarily reflect the position or the policy of the Government, and no official endorsement should be inferred.

Abstract

An acoustic min-drifting buoy designed to meet operational naval demands for real time monitoring of upper ocean air/sea interface processes is described. The AN/WSQ-6 (XAN-2) acoustic drifting buoy is an air-deployable, standard sonobuoy-sized buoy. When deployed, a hydrophone suspended below a small surface float. Data collected by the system are transmitted to users via ARGOS satellite link. Atmospheric pressure, air and sea temperature, and ambient sound levels are measured directly. Indirect measurements of wind speed and precipitation are made using the ambient sound field data.

1. Introduction

Real time observations of air/sea conditions are needed as input into operational models predicting the performance of naval sensors and systems in the near surface ocean and atmosphere. Often, the regions where these measurements are needed are remote and are difficult or dangerous locations to operate traditional observation platforms. Consequently, an operational requirement for expendable, satellite-reporting drifters was issued by the Oceanographer of the Navy, OR #276-096-91.

Expendable autonomous drifting buoys, the AN/WSQ-6 series, have recently been developed by the U.S. Navy to provide these real-time measurements of upper ocean conditions (Selsor, 1993). One AN/WSQ-6 buoy configuration, XAN-2, monitors temperature, atmospheric pressure and ambient noise levels directly. Other important air/sea processes, such as wind speed/stress, sea state and precipitation are inferred by analyzing the ambient sound produced by these processes. This buoy configuration is also known as an ambient noise sensor (ANS) drifter.

2. Background: Underwater Sound Generation by Wind and Rain

Mechanical devices designed to measure wind and precipitation perform poorly in oceanic deployments because of fouling and platform problems. Fortunately, these same processes generate sound underwater and this sound can be used as a signal to quantitatively measure wind speed and rainfall rate. Figure 1 presents generic underwater spectral acoustic signatures of various air/sea interaction phenomena. Because each of these phenomena possess different acoustic signatures, Shaw *et al.*, (1978) proposed making geophysical measurements of wind speed (stress) and precipitation using passive underwater ambient noise sensors.

Wind speed has been associated with underwater sound levels since Knudsen et al. (1948). Evans et al., (1984) and Lemon et al., (1984) documented the ability to measure wind speed using ambient sound. The source of sound generation by wind are breaking wind waves (Farmer and Vagle, 1988). At high frequencies (above 500 Hz), acoustic radiation from newly created individual bubbles within the whitecap can be used to explain the observed spectral signature of wind (Medwin and Beaky, 1989). At lower frequencies, the collective oscillation of bubble clouds have been observed to radiate sound (Loewen and Melville, 1994). Vagle et al. (1990) proposed a generalized algorithm for inferring wind speed from ambient sound measurements. This algorithm includes flags for precipitation and shipping, two other dominant (but fortunately intermittent) noise sources in the frequency bands being used to measure wind (1-15 kHz).

The Vagle et al. (1990) algorithm was evaluated by Dailey (1991). Data from two prototype acoustic drifters deployed off of the California coast were compared with wind speed fields observed using the Defense Meteorological Satellite Program (DMSP) Special Scanning Microwave Imager (SSM/I) (Goodberlet et al. 1989). Good agreement between the acoustical and satellite measurements were observed. The correlation coefficient was $r \sim .8$ and the slope of the linear regression was near 1 (Dailey, 1991). The scatter observed was similar to the scatter observed during comparison of wind speed from buoys and SSM/I wind speed estimates (Goodberlet et al. 1989).

Rain is another dominant source of underwater sound (Heindsman et al., 1955). Laboratory studies have identified the sound production mechanisms associated with raindrop splashes (Franz, 1959; Pumphrey *et al.* 1989; Medwin et al., 1992; Nystuen and Medwin, 1995). There are two raindrop sizes that are important for underwater sound generation. These are "small", 0.8-1.1 mm diameter, and "large", 2.2-4.6 mm diameter raindrops. These two drop sizes regularly trap bubbles, an extremely effective sound generator, underwater during the raindrop splash. Because of different size distributions of the bubbles created by these two drop sizes,

different underwater sound spectra are generated by light rain (containing only small drops) and heavy rain (containing both small and large drops).

Wind has been shown to strongly affect the sound produced by light rain (Nystuen and Farmer, 1987; Nystuen, 1993) and consequently quantitative estimates of rainfall rate from light rain without knowledge of the wind conditions are unlikely. On the other hand, detection of light rain is possible, even in high sea states (Nystuen and Farmer, 1989). In the case of heavy rain, the sound produced is independent of wind speed, at least for wind speeds less than 10 m/s (Nystuen *et al.*, 1993) and so detection and quantification of rainfall rate is possible. Furthermore, since each raindrop size produces sound with unique spectral characteristics, the sound spectrum can be inverted to measure raindrop size distribution (Nystuen, 1995). Dailey (1991) verified detection of rainfall from acoustic drifters at times when SSM/I rainfall rate fields indicated rainfall over the buoys.

One additional measurement from acoustic drifters is likely. Farmer and Lemon (1984) report that for wind speeds above 10 m/s, relatively low sound levels are observed at frequencies above 10 kHz (when compared to 4 kHz). They suggest that this is due to attenuation of surface generated sound passing through ambient bubble clouds. Because acoustical attenuation by bubbles is frequency dependent, bubble populations can be estimated by measuring the apparent attenuation. Nystuen *et al.* (1993) show a similar effect during extremely heavy rainfall. By measuring the sound field at two depths, near the surface (≈1 m) and below the bubble cloud layer (≈ 10 m), integrated bubble populations can be estimated. These bubbles affect sound speed and acoustical reverberation at the ocean surface and consequently modify sound propagation in the surface sound duct. Furthermore, they are an indication of turbulent mixing in the near surface layer.

3. AN/WSQ-6 XAN-2 (or ANS Drifter) Buoy Description

The AN/WSQ-6 buoy system fits inside a standard A-size sonobuoy canister (Fig. 2). It is certified to be air deployed using a standard sonobuoy chute for air speed under 300 knots. As the canister leaves the airplane, the end cap is pulled off and a parachute deploys. Upon contact with seawater, the seawater electrode triggers the gas cylinders to discharge, inflating the floatation collar, deploying the antenna and dropping the hydrophone package (hydrophone, drogues, weight and cable). The physical configuration of a deployed buoy is shown in Fig. 3.

The drogues are designed to decouple the motion of the surface buoy from the hydrophone, located at the lowest drogue. This is required to reduce flow noise, which would be detected as noise at frequencies below 100 Hz. The drogues produce a 17:1 drogue/cable to surface buoy drag ratio, thus providing limited Lagrangian drifter characteristics.

The pressure sensor is a low-cost, temperature compensated strain gauge with dynamic range 850-1054 mb ± 1 mb (McCormick *et al.*, 1990). The pressure port, covered with a Gore-Tex splash guard, is at the top of the antenna mast to reduce problems with splash and submergence. The strain gauge itself is located at the bottom of the drifter hull, below the water line, to improve temperature stability.

The air temperature sensor, shielded from direct sun, is located near the top of the mast. It has a range of -30° to 46°C ± 0.2°C. The surface water temperature sensor is incorporated into the base of the buoy hull. Its range and sensitivity is -5 to +35°C ± 0.2°C. Performance characteristics were verified by McCormick *et al.* (1990).

The ambient sound sensor is an omni-directional (± 1 dB below 10 kHz; ± 3 dB from 10-25 kHz) hydrophone located at the lowest drogue at 100 m depth. The acoustic data is sampled once per hour through 16 third octave band pass filters with center frequencies from 5 Hz to 25 kHz. The signal from each third octave filter is converted to a DC voltage using a root mean square circuit and is digitized using a 16-bit analog-digital

circuit. The resulting dynamic range is 9 orders of magnitude in acoustic intensity (35 -125 dB ± 2 dB relative to 1 mPa^2/Hz from 5 Hz to 5 kHz and 20 - 110 dB ± 2 dB relative to 1 mPa^2/Hz from 8 kHz to 25 kHz).

Data from the pressure, temperature and ambient sound sensors are stored in six 32-bit data blocks and broadcast by the ARGOS satellite transmitter every 90 seconds. Depending on the buoy latitude, satellites are in position to receive the ARGOS transmission 8-12 times per day. The ambient noise data is updated once per hour while data from the other sensors are updated every 10.5 minutes. Only the latest data are transmitted.

4. Example of Data Collection from an ANS Drifter

In April 1992, an ANS drifter was deployed at 33.7°N, 66.4°W. Fig. 4 shows the drifter position during the first 30 days of operation. A strong atmospheric front passed over the drifter on Julian Days 119 and 120. The acoustic suspension system broke after this storm and thereafter only surface sensor data (air, sea temperature and barometric pressure data) were available. Fig. 5 shows surface pressure charts during the passage of the weather front on JD 119/120. Fig. 6 shows the barometric pressure and temperature records from the drifter. The frontal passage is easily detected in the barometric pressure record and shows values consistent with the surface pressure charts. The air temperature record shows a diurnal heating pattern except during the frontal passage on JD 120.

Figure 7 shows the acoustic spectra (80 spectra) recorded during nine days of deployment, including the time period corresponding to the passage of the atmospheric front depicted in Fig. 5. The sound levels range over seven orders of magnitude in intensity, with the highest levels prevalent below 100 Hz. A persistent maximum is present in the spectra at 50 Hz. This is a frequency dominated by distant shipping noise. Unusually high sound levels at this frequency are likely to be nearby ships, especially if other higher frequency channels simultaneously show high levels. The sound level at 5 Hz is variable and, in fact, will be shown to be correlated to the higher frequency (above 500 Hz) channels. Two spectra which stand out above 500 Hz are labeled "rain". These spectra were recorded during heavy rainfall as verified by satellite data and demonstrate that rainfall dominates the underwater sound spectrum above 500 Hz when it is present.

Above 500 Hz, Fig. 8, the spectra are known to be correlated with wind speed. The spectral slopes are relatively uniform and the spectra are generally offset from one another. The intensity level at any given frequency can be related to wind speed. Vagle et al. (1990) published an acoustic wind algorithm using the sound intensity at 8 kHz. Some deviations from a uniform spectral slope are apparent. The loudest spectra show spectral slope steepening above 10 kHz. This is due to ambient bubble clouds which attenuate sound at the highest frequencies (Farmer and Lemon, 1984). The quietest spectra show a flattening of the spectra above 2 kHz. This is apparently the shape of the ambient background noise field for this part of the ocean.

An examination of the time histories of the sound intensity at six selected frequencies (Fig. 9) shows that on several occasions the sound levels increase abruptly at all frequencies except 25 kHz, e.g. on JD 114 and 116. Nearby shipping (as opposed to distant shipping) would produce this signal. The typical propagation path from the ship to the drifter is horizontal. Higher frequency sound is attenuated more strongly by sea water, causing a "reddening" of the spectrum. For distant shipping, only low frequency sound is detected, i.e. at 50 Hz. For nearby shipping, higher frequencies are also elevated. On JD 118, an abrupt increase is observed at all frequencies, including 25 kHz. If this is ship induced, then the ship must have passed very close to the drifter.

On JD 120, a very loud signal is detected from 200 - 25000 Hz. This is a heavy rainfall event associated with the frontal passage. Note that there is no signal from this event at 10 and 50 Hz. There is no physical mechanism for rain to produce such low frequency sound.

Except for an occasional ship, the sound levels between 10 and 200 Hz are poorly correlated to the sound level at 5 Hz and above 500 Hz. This is depicted graphically in Figure 10. Fig. 10 shows the correlation of each frequency (16 curves) with all of the other frequencies. By definition, the correlation of each frequency with itself is one and so each line can be identified (only 4 lines are labeled). The group of curves banded together are the 10 frequency channels from 500 Hz to 25 kHz. These high frequencies (spectra shown in Fig. 8) are highly correlated to wind speed, and thus with each other. The lowest frequency band, 5 Hz, is also relatively highly correlated to the high frequencies. This high correlation is probably an indication of incomplete decoupling of the surface buoy from the hydrophone, i.e., the hydrophone is sensing the surface wave field through the surface buoy. The other low frequency channels (10-200 Hz) are poorly correlated with all other channels. This suggests that sound sources in this frequency range are relatively narrow band, rather than broad band.

5. Data analysis - Interpretation of the Ambient Sound Field

A. Algorithm to identify sound source (wind, rain, drizzle, shipping)

Different underwater sound sources have different spectral shapes (Fig. 1). These differences allow an automated algorithm to be designed to determine which process is dominating the sound field at any moment in time. Above 500 Hz, four sound sources need to be identified: wind, rain, drizzle and shipping. Of these, wind is the most obsequious. The others occur relatively infrequently. Another phenomena that affects the shape of the sound spectrum are extensive bubble clouds. This can be called "high sea state" as it is an indication of extensive wave breaking.

The flow chart for a decision making algorithm is shown in Figure 11. One method to try to identify spectral shape is to calculate a mean spectral slope and then compare the expected slope for wind speed. A second method is to calculate spectral differences between selected frequencies. These frequencies are chosen to optimize detection of the unique known features of the sound sources, e.g., the 13-20 kHz spectral peak of drizzle.

Figure 12 shows the calculation of mean spectral slope between 500 and 25000 Hz for ANS drifter #14359. In general the slope is inversely proportional to the higher frequency sound levels. When the sound levels are low, the slope is low (JD 115) and when sound levels are high, the slope is steep (JD 121). A few abrupt changes are detected (JD 114, JD 116 and JD 118). These are likely shipping detections. The steepened slope on JD 121 is likely due to bubble cloud attenuation of the sound levels above 10 kHz, i.e., a high sea state (extensive wave breaking) is present.

The characteristic feature of the wind generated spectrum is the relatively uniform slope. Vagle et al. (1990) reported a value of -19 dB/decade and proposed to detect "wind" when the observed slope was within ± 3 dB/decade of this value. It is clear from Fig. 12 that the slope value can deviate from -19 dB/decade. In fact, given the correlation of the slope to the higher frequency acoustic intensities and the fact that thse frequencies are correlated to wind speed, the assumption that the slope is independent of wind speed is questionable. Dailey (1991) showed that "wind" spectral values varied from -19 dB/decade to -27 dB/decade. He proposed that ± 3 dB/decade departures from a two-day running mean be used to detect "non-wind" sound sources. While this modification may "detect" sudden events (a passing ship or heavy rain), it does not allow for sudden changes in the wind.

The alternate method to obtain sound source classification is to compare the spectral levels at selected frequencies. Figure 13 shows a comparison of spectral levels at 5 and 25 kHz. Most points fall along a fairly well defined curve. These are assumed to be "wind" spectra, the most obsequious sound source. As the wind increases, wave breaking increases the sound intensity at both frequencies in a well defined stretched s-shaped

pattern. At the "quiet" end of these data points, the sound levels approach the background noise level for 25 kHz more quickly than at 5 kHz. Thus, the flattening of the curve. This feature is likely to be location dependent. At the "loud" end, bubble clouds attenuate the 25 kHz sound levels, but do not affect the sound at 5 kHz. Thus, as sea state increases, the sound at 5 kHz continues to increase but can actually decrease at 25 kHz (Farmer and Lemon, 1984). This is because bubbles selectively attenuate sound at their resonance frequency. Few bubbles of the size needed to attenuate 5 kHz are present in the ambient bubble field (they are too big), while many smaller bubbles (which attenuate higher frequencies) are present. Data points falling on this portion of the "wind" curve indicate "high sea state".

Other sound source changes the sound intensities in very different ways. For example, ships increase the low frequency sound level more relative to the high frequency channel. Thus, "shipping" is detected when data points fall below the "wind" curve. Drizzle produces excess sound at high frequencies and is therefore detected when data points fall above the "wind" curve. Heavy rain produces very loud levels at all frequencies and is detected by data points falling well above the curve. The dividing line between drizzle and heavy rain is difficult to establish.

B. Quantification of wind speed and rainfall rate

Once the sound source has been identified, quantification is possible. Two algorithms are presently available: wind speed (Vagle et al., 1990) and heavy rain (Nystuen et al., 1993). The wind speed algorithm can be applied except when "shipping" or "heavy rain" are detected. These two sound sources obscure the sound from wind and, thus, make wind speed estimates impossible.

The Vagle et al. (1990) wind speed algorithm uses the sound level at 8 kHz and is given by:

$$P_0 = 10^{\left(\frac{SSL_0}{20}\right)}$$

$$V = \frac{P_0^2 - b}{a}$$

where SSL_0 is the sound spectrum level at 8 kHz in dB relative to 1 mPa^2/Hz, P_0 is a non-dimensional pressure, a = 53.91 and b = -104.5 are linear regression coefficients and V is the wind speed at 10 m above the ocean in m/s.

Figure 14 shows the acoustic wind speed estimates for Drifter #14359. Comparison data are supplied by passive microwave satellite data from the DMSP Special Scanning Microwave Imager (SSM/I). The agreement is remarkably good. The passage of the front on JD120 included a period of low wind, followed by relatively high winds and high sea states. The acoustic wind speed record has much better temporal resolution than the satellite data. At a specific location, satellite data is not available every day. Furthermore, for sun-synchronous satellites, the data is always recorded at the same local time. Of course, satellites provide large scale spatial resolution. The spike in wind speed on JD118 is probably an incorrectly classified "ship".

ANS wind speed data has been recorded for several other test deployments. The deployments were in the North Atlantic, North Pacific and Gulf of Mexico. These data are combined in Figure 15. The correlation between the acoustic and satellite wind speed estimates is r = 0.91. There is a tendency for the acoustic measurement to be biased low, however there is not enough data to make a definative statement. Dailey (1991)

reported good agreement between acoustic and SSM/I wind speed estimates in off the coast of California (r = 0.84). He also reported a bias towards low wind speed estimates for the acoustic method in warmer sub-tropical Pacific water.

While both drizzle and heavy rainfall can be detected acoustically, only heavy rainfall can be quantified. This is because the signal for drizzle is strongly affected by wind speed (Nystuen, 1993). The Nystuen et al. (1993) heavy rainfall rate algorithm is given by:

$$RR = 10^{\frac{SSL_{5.5kHz} - 53.29dB}{10.59}}$$

where $SSL_{5.5\,kHz}$ is the sound spectral level at 5.5 kHz in dB rel 1 mPa^2/Hz. Figure 16 shows the two "heavy rain" detections during the frontal passage for Drifter #14359. The spectra are shown along with the rainfall rate estimates. Also shown are the two "wind only" spectra immediately preceeding and following the rain spectra. Verification of the rainfall estimate is extremely difficult for two reasons. First, co-located satellite passes are very infrequent and, second, quantitative estimates of rainfall rate from satellites are very questionable. In fact, this particular rainfall detection was verified by a SSM/I satellite pass 1 minute before the acoustic spectrum (Fig. 17). "Heavy" rain is indicated by the satellite, however this value is only 5 mm/hr. The acoustic estimate of 63 mm/hr is more likely to be closer to the truth; the sound levels are very high. For rainfall detection and measurement, the liabilities of the satellite are significant. Not only is the temporal sampling poor, the spatial footprint of the satellite is very large relative to the size of the rain. Thus, rainfall is inhomogeneous within the footprint of the satellite sensor. For the acoustic drifters, the effective listening area for high frequency sound is roughly 100 m in diameter centered over the hydrophone.

Recently, an improved acoustic algorithm for rainfall rate estimation has been developed (Nystuen, 1995). This algorithm has not been adapted for use on acoustic drifters.

6. Conclusions

Acoustic mini-drifting buoys have been developed to monitor upper ocean air/sea interface processes in real time. These buoys are air-deployable, standard sonobuoy-sized instruments. When deployed, a hydrophone is suspended below a small surface float. Data collected by the system are transmitted to users via the ARGOS satellite communication link. Atmospheric pressure, air and sea temperature, and ambient sound levels are measured directly. The ambient sound field can be further interpreted to measure wind speed, sea state and precipitation.

Observations from a month long deployment of a drifter in the North Atlantic show reasonable temperature and pressure records during the passage of a strong front. The observations are in agreement with standard weather charts, although no *in situ* temperature and pressure observations were available for comparison.

The acoustic records also detect the passage of the atmospheric front. The sound levels between 500 Hz and 25 kHz (10 channels) are very highly correlated to one another indicating that these frequencies are all responding to the wind field. The signal at 5 Hz is also significantly correlated to the higher frequencies. This is probably an indication of incomplete de-coupling of the surface float and the hydrophone, i.e. the influence of surface waves on the float are being transmitted through the compliance system to the hydrophone location. The motion of the hydrophone is then detected as a signal at 5 Hz. The signal between 10 Hz and 100 Hz (4

channels) are decorrelated to all other frequency bands indicating that the sound sources from 10-100 Hz are narrow band and independent of the local wind field.

The sound field from 500 Hz to 25 kHz can be used to measure wind speed, sea state and precipitation. An algorithm used to identify the sound source (wind, drizzle, heavy rain or ship) is described and demonstrated. The acoustic wind speed measurements are shown to be in excellent agreement with satellite wind speed estimates. The acoustic system has much higher temporal resolution than the satellite system. Rainfall detection is also demonstrated and compared to a satellite detection of heavy rain. The satellite estimate is much lower than the acoustic estimate. This probably reflects the limitations of satellite rainfall quantification; the acoustic estimate of rainfall rate is likely the better estimate.

7. Acknowledgements

The AN/WSQ-6 buoy development program is sponsored by the Oceanographer of the Navy (OP-096) who has issued an operational requirement, OR #276-096-91, for monitoring upper ocean processes using expendable buoys. The program is managed by the Tactical Oceanography Warfare Support (TOWS) program office, Naval Research Laboratory- Detachment, Stennis Space Center, Mississippi. The scientific officer is Harry D. Selsor. Metocean Data Systems Ltd. of Dartmouth, Nova Scotia developed and built the AN/WSQ-6 drifters.

References

Dailey, C.H., "Analysis of wind and rainfall measurements from acoustic drifters", Master's Thesis, Naval Postgraduate School, Monterey, CA 93943 (1991).

Evans, D.L., D.R. Watts, D. Halpern and S. Bourassa, "Oceanic winds measured from the seafloor", J. Geophys. Res. **89**, 3457-3461 (1984).

Farmer, D.M. and D.D. Lemon, "The influence of bubbles on ambient noise in the ocean at high wind speeds" J. Phys. Ocean. **14**, 1762-1778 (1984).

Farmer, D.M. and S. Vagle, "On the determination of breaking wave distributions using ambient sound" J. Geophys. Res. **93**, 3591-3600 (1988).

Franz, G., "Splashes as sources of sound in liquids", J. Acoust. Soc. Am. **31**, 1080-1096 (1959).

Goodberlet, M.A., C.T. Swift, and J.C. Wilkerson, "Remote sensing of ocean surface winds with the special sensor microwave/imager", J. Geophys. Res. **94**, 14547-14555 (1989).

Heindsman, T.E., R.H. Smith and A.D. Arneson, "Effect of rain upon underwater noise levels", J. Acoust. Soc. Am. **27**, 378-379 (1955).

Knudsen, V.O., R.S. Alford and J.W. Emling, "Underwater ambient noise", J. Mar. Res. **1**, 410-429 (1948).

Lemon, D.D., D.M. Farmer and D.R. Watts, "Acoustic measurements of wind speed and precipitation over a continental shelf", J. Geophys. Res. **89**, 3462-3472 (1984)

Loewen, M.R. and W.K. Melville, "An experimental investigation of the collective oscillations of bubble plumes entrained by breaking waves", J. Acoust. Soc. Am. **95**, 1329-1343 (1994).

McCormick, M.J., R.L. Pickett and G.S. Miller, "A field evaluation of new satellite-tracked buoys: A LORAN-C position recording and a sonobuoy type drifter", MTS Journal **25**, 29-33 (1990).

Medwin, H. and M.M. Beaky, "Bubble sources of the Knudsen sea noise spectra", J. Acoust. Soc. Am. **86**, 1124-1130 (1989).

Medwin, H., J.A. Nystuen, P.W. Jacobus, D.E. Snyder and L.H. Ostwald, "The anatomy of underwater rain noise", J. Acoust. Soc. Am. **92**, 1613-1623 (1992).

Nystuen, J.A., "An Explanation of the Sound Generated by Light Rain in the Presence of Wind", in Natural Physical Sources of Underwater Sound, ed. B.R. Kerman, Kluwer Academic Publishers, 659-668 (1993).

Nystuen, J.A., "Acoustical Rainfall Analysis: Rainfall drop size distribution using the underwater sound field", J. Atmos. and Oceanic Tech. (1995).

Nystuen, J.A., C.C. McGlothin and M.S. Cook, "The Underwater Sound Generated by Heavy Precipitation", J. Acoust. Soc. Am. **93**, 3169-3177 (1993).

Nystuen, J.A. and D.M. Farmer, "The Influence of Wind of the Underwater Sound Generated by Light Rain", J. Acous. Soc. Am. **82**, 270-274 (1987).

Nystuen, J.A., and H. Medwin, "Underwater Sound Generated by Rainfall: Secondary Splashes of Aerosols", J. Acoust. Soc. Am. **97**, 1606-1613 (1995).

Pumphrey, H.C., L.A. Crum and L. Bjorno, "Underwater sound produced by individual drop impacts and rainfall", J. Acoust. Soc. Am. **85**, 1518-1526 (1989).

Selsor, H.D., "Data from the sea: Navy Drifting Buoy Program", Sea Technology **34**, 53-58 (1993).

Shaw, P.T., D.R. Watts and H.T. Rossby, "On the estimation of oceanic wind speed and stress from ambient noise measurements", Deep Sea Research **25**, 1225-1233 (1978).

Vagle, S., W.G. Large and D.M. Farmer, "An evaluation of the WOTAN technique for inferring oceanic winds from underwater sound", J. Atmos. and Oceanic Tech. **7**, 576-595 (1990).

List of Figures

Figure 16. Acoustic detection of heavy rain from Drifter #14359. Two "wind only" spectra (at 0555z and 1208z) are also shown. The quantitative estimates of rainfall rate use the algorithm of Nystuen et al. (1993). The wind speed is estimated using the algorithm of Vagle et al. (1990).

Figure 17. The microwave (SSM/I) satellite image for rainfall rate one minute prior (at 0913z) to the acoustic rainfall detection (at 0914z) on JD 120.

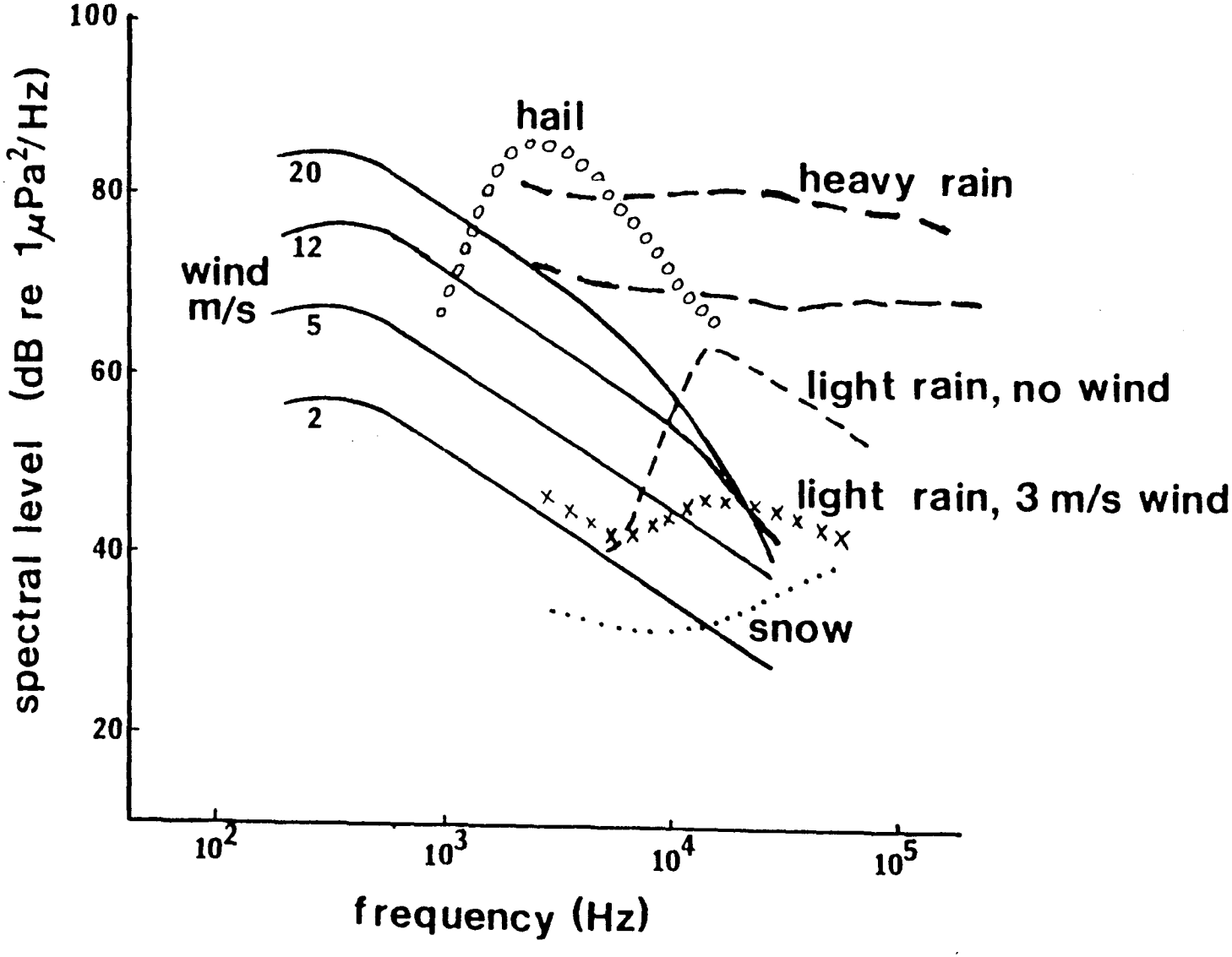

Figure 1. Generic underwater sound spectra for different air/sea physical processes.

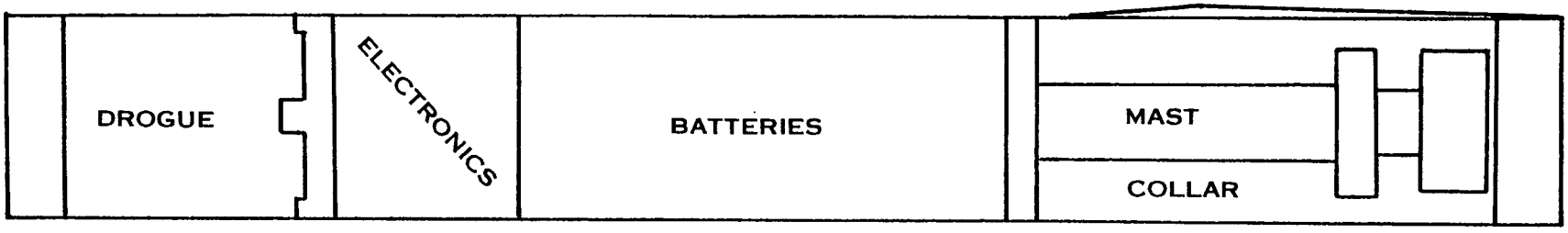

Figure 2. Physical configuration of an AN/WSQ-6 acoustic drifter in a standard A-Sized sonobuoy canister.

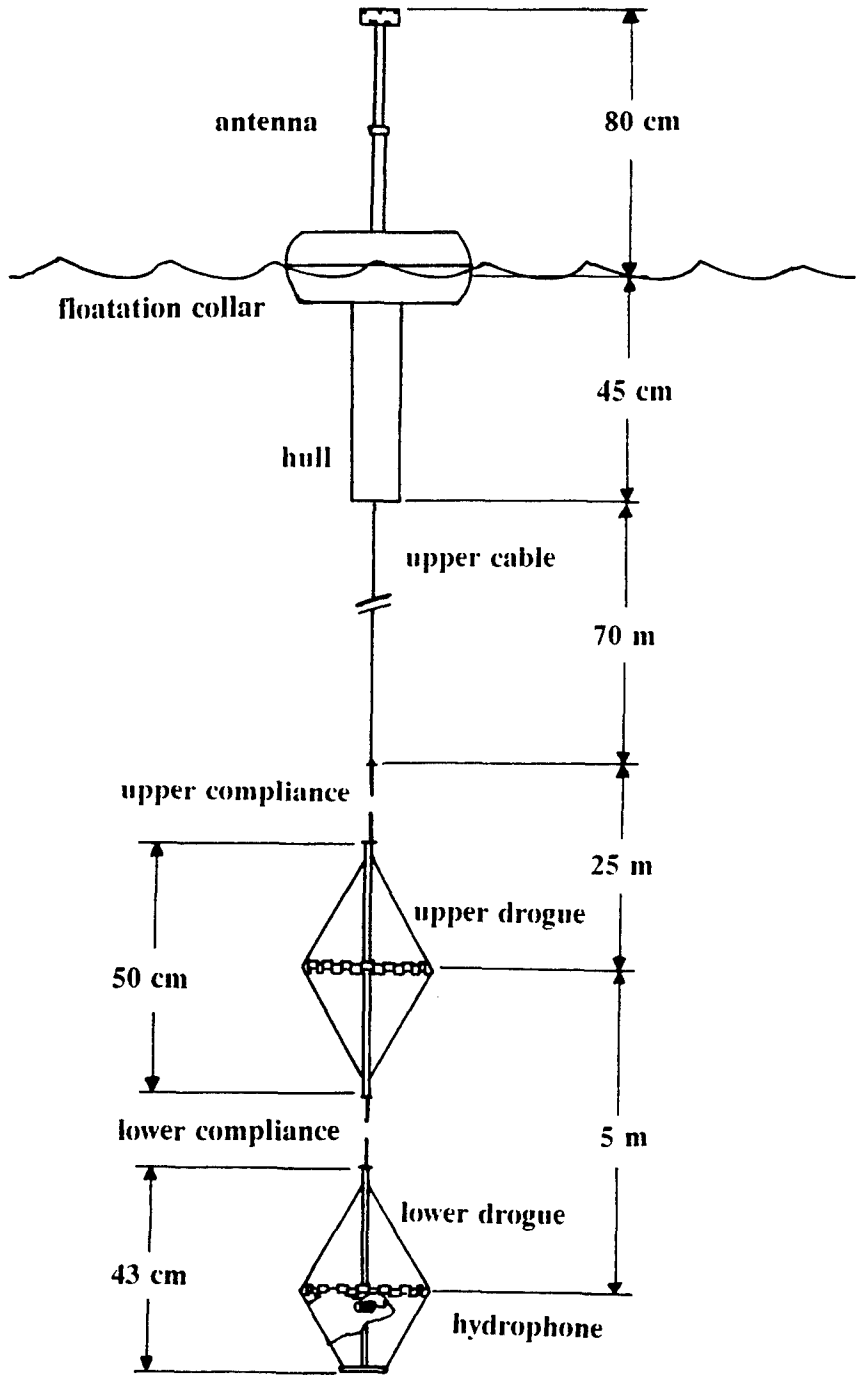

Figure 3. Deployed configuration of an AN/WSQ-6 acoustic drifter.

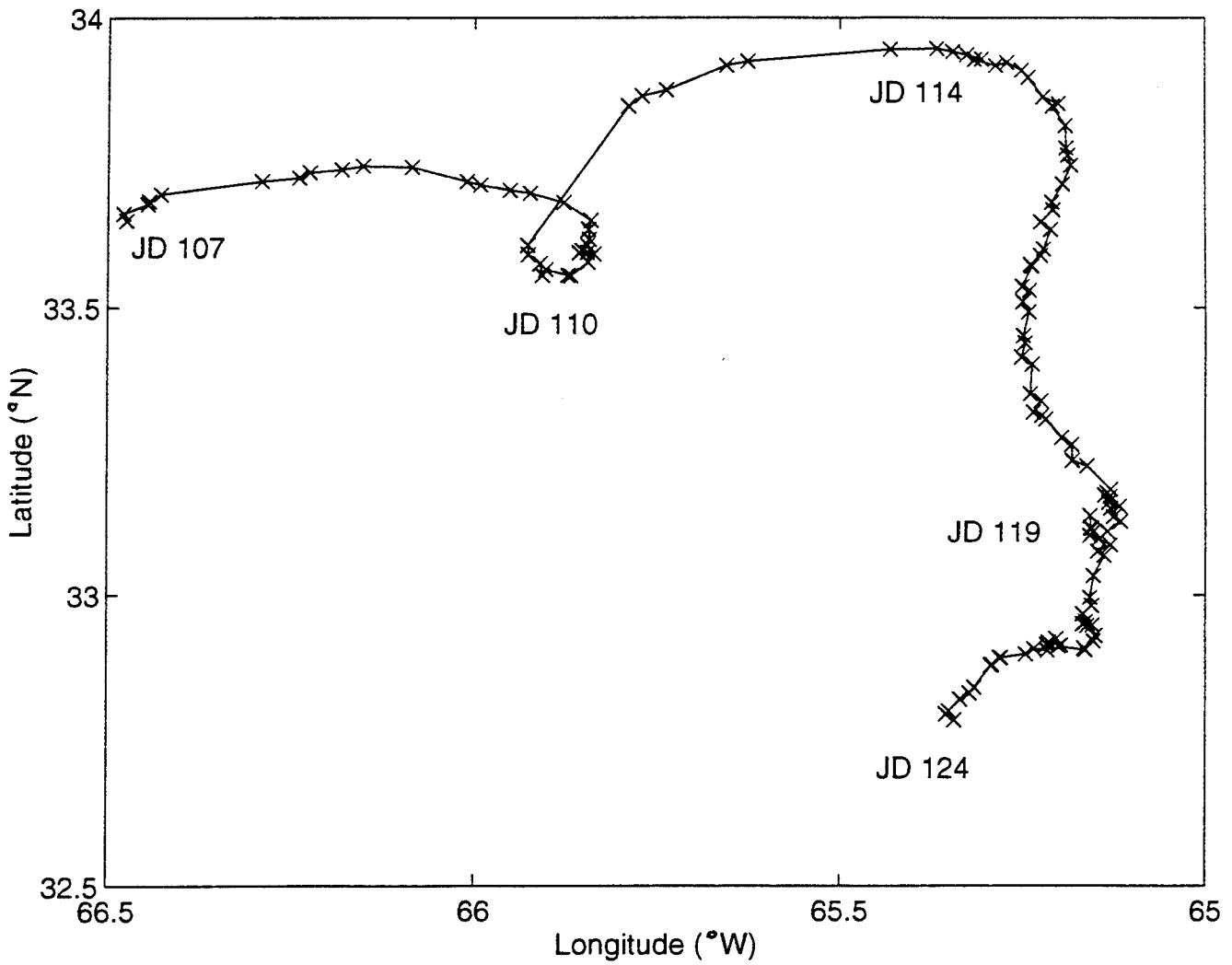

Figure 4. Drifter #14359 position in the North Atlantic from Julian Day (JD) 107 to JD 124. 1992. The X symbols show individual location fixes from the ARGOS positioning system.

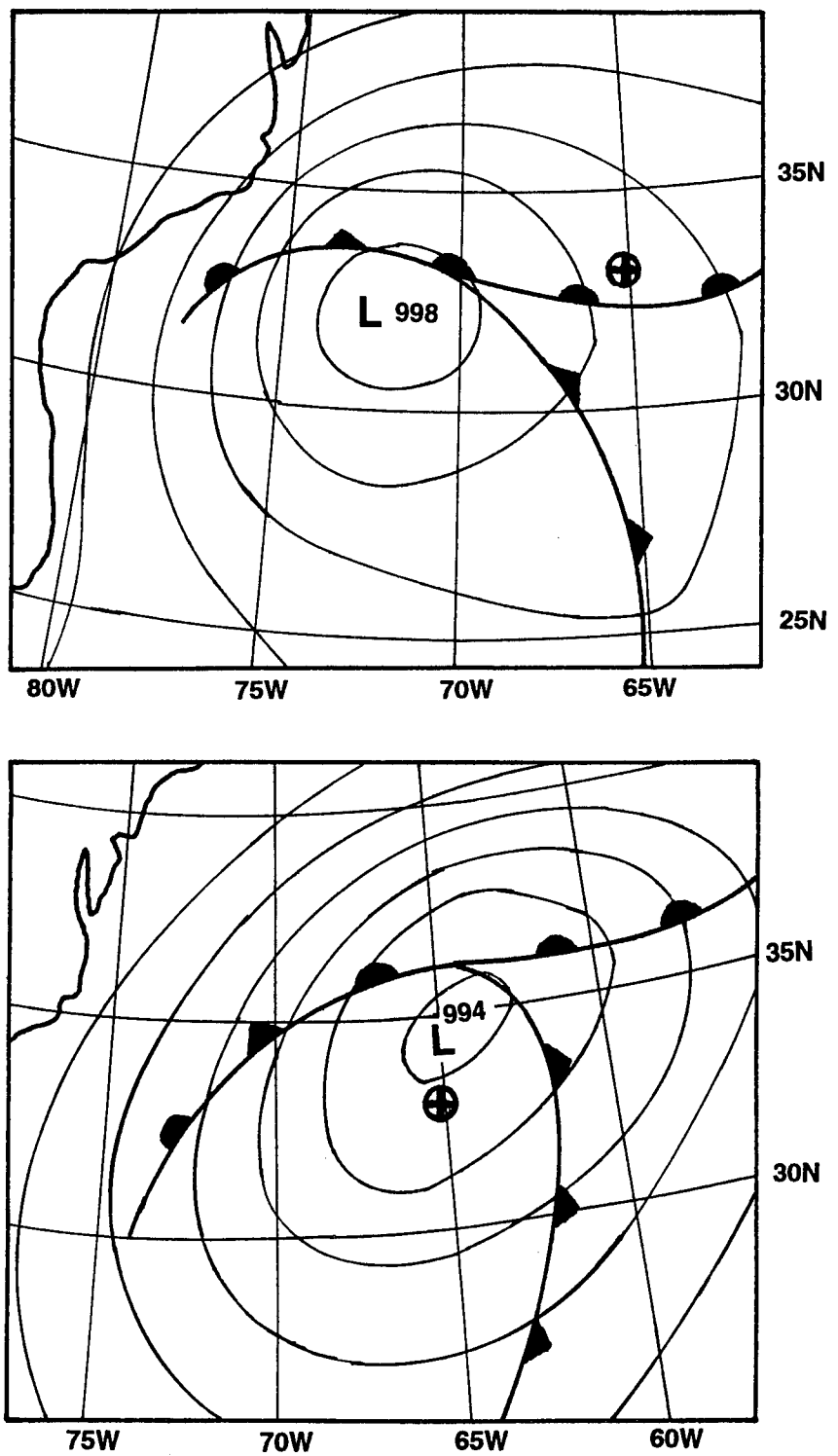

Figure 5. Surface pressure charts for a storm passage over the Drifter #14359 on JD 119/120 1992. The ⊕ symbol shows the buoy location.

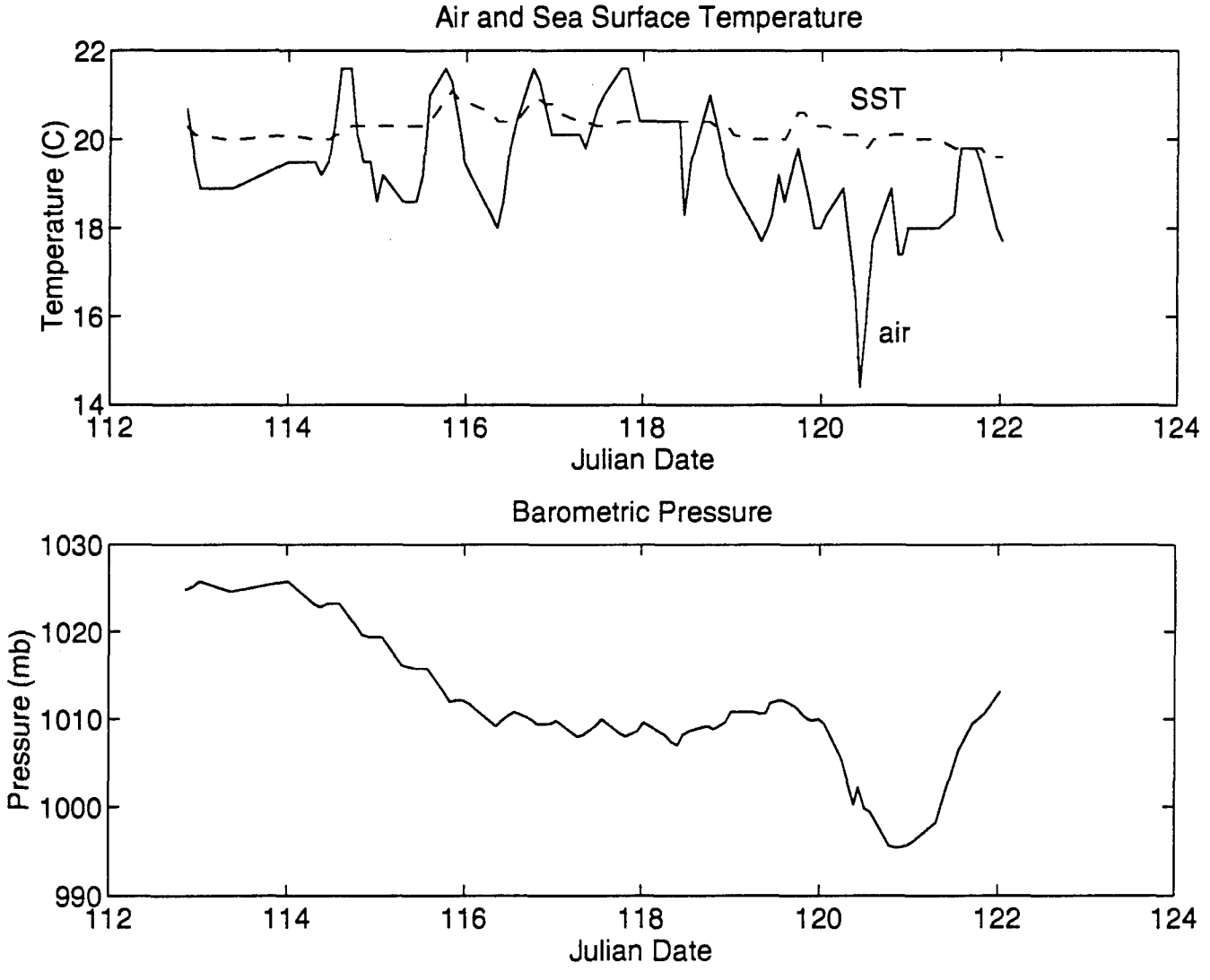

Figure 6. Barometric surface pressure and temperature (air and sea) from Drifter #14359. Note the storm passage on JD 120.

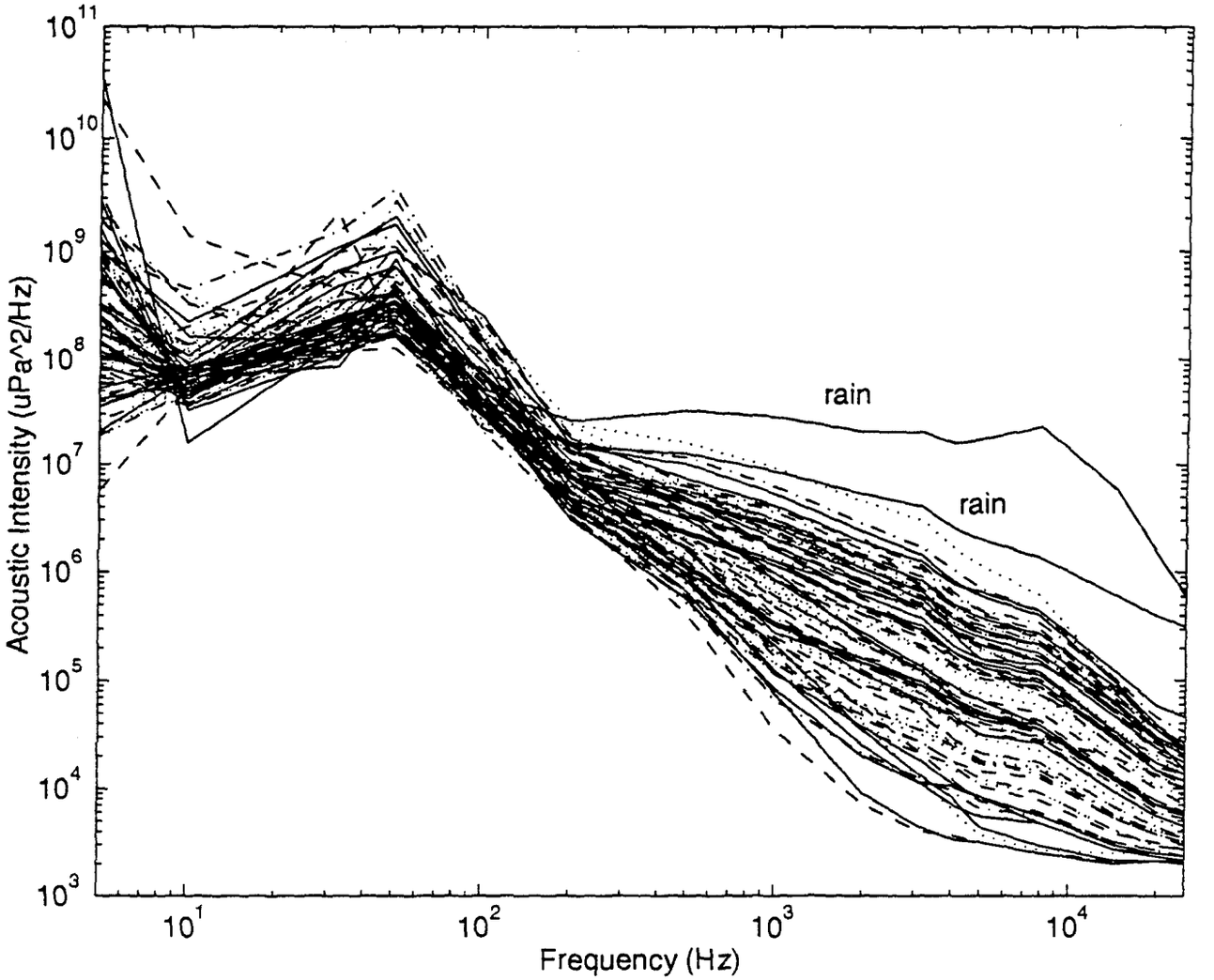

Figure 7. Eighty acoustic spectra recorded during the deployment of Drifter #14359.

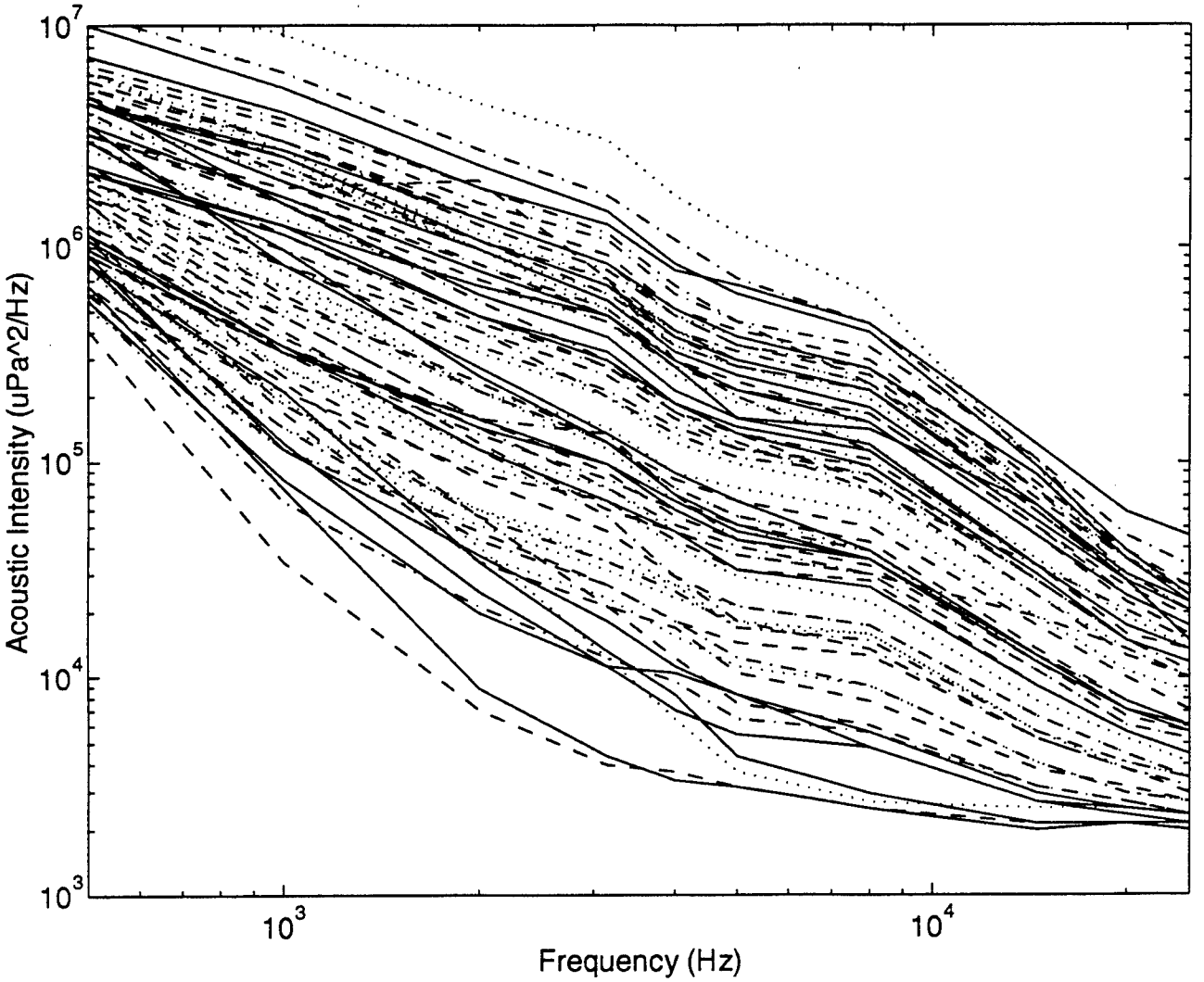

Figure 8. Acoustic spectra from 500 Hz to 25 kHz.

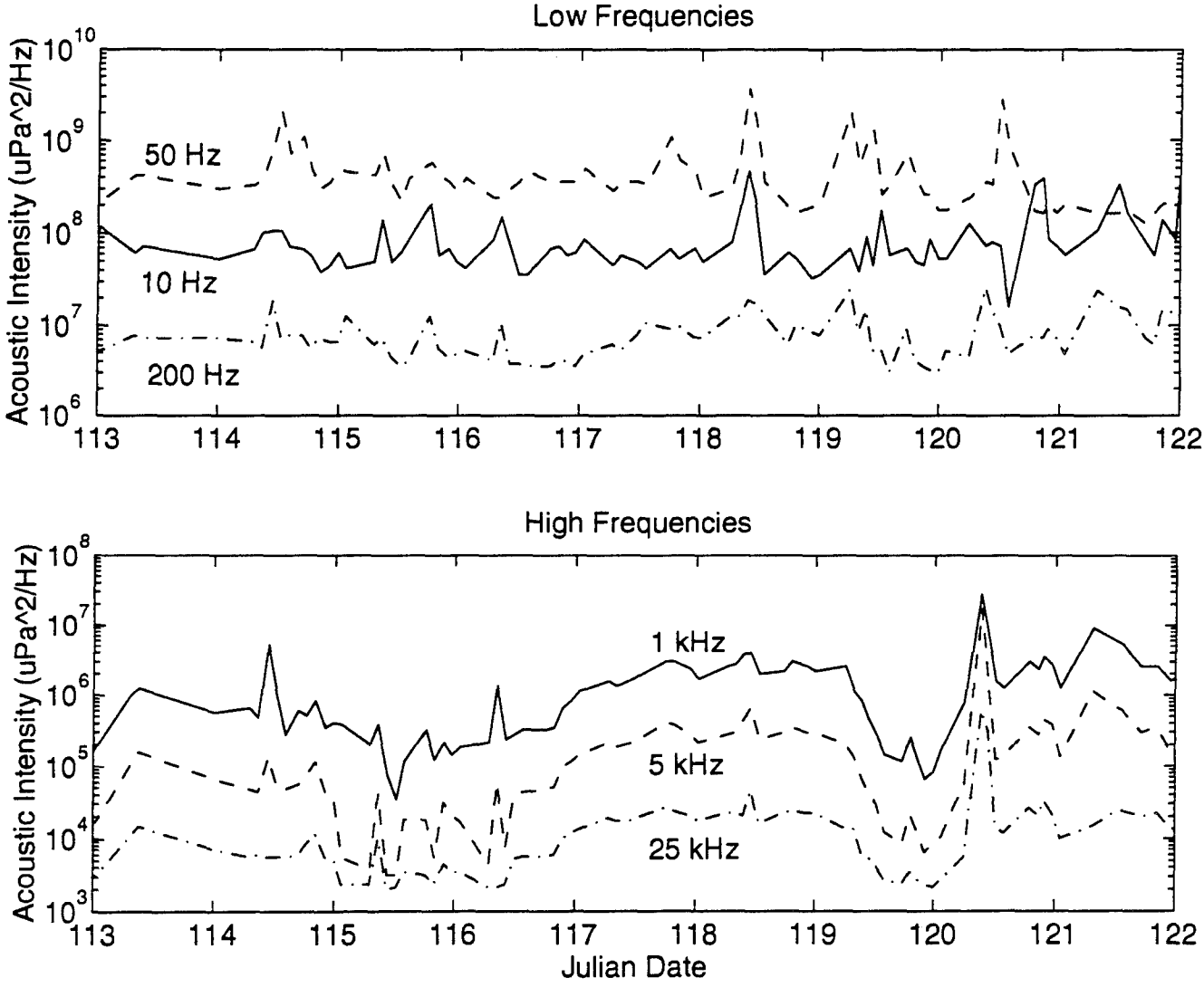

Figure 9. Time series of sound intensity at selected frequencies. Close ship passages affect the sound intensity at all frequencies. Examples are during JD 114, 116 and 118. Rain only affects the higher frequencies. An example is during JD 120.

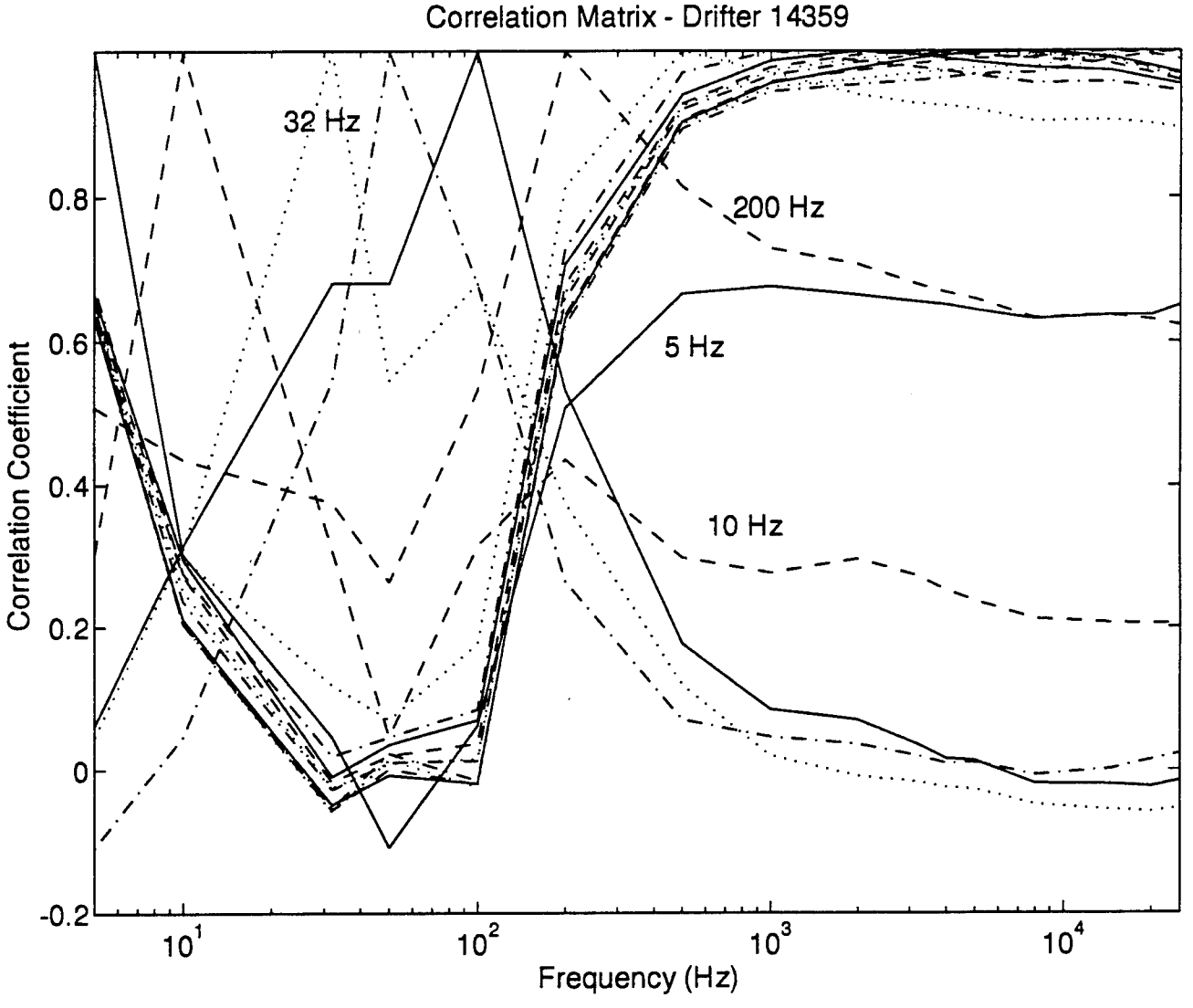

Figure 10. The intercorrelation of each frequency band with all other frequency bands. Only four lines are labeled. The cluster of lines are the ten channels from 500 Hz to 25 kHz. These channels are highly correlated with each other, indicating that the same physical processes affect these channels in similar fashion. The channels between 10 Hz and 100 Hz are poorly correlated with all other channels indicating narrow band sound sources over this frequency range.

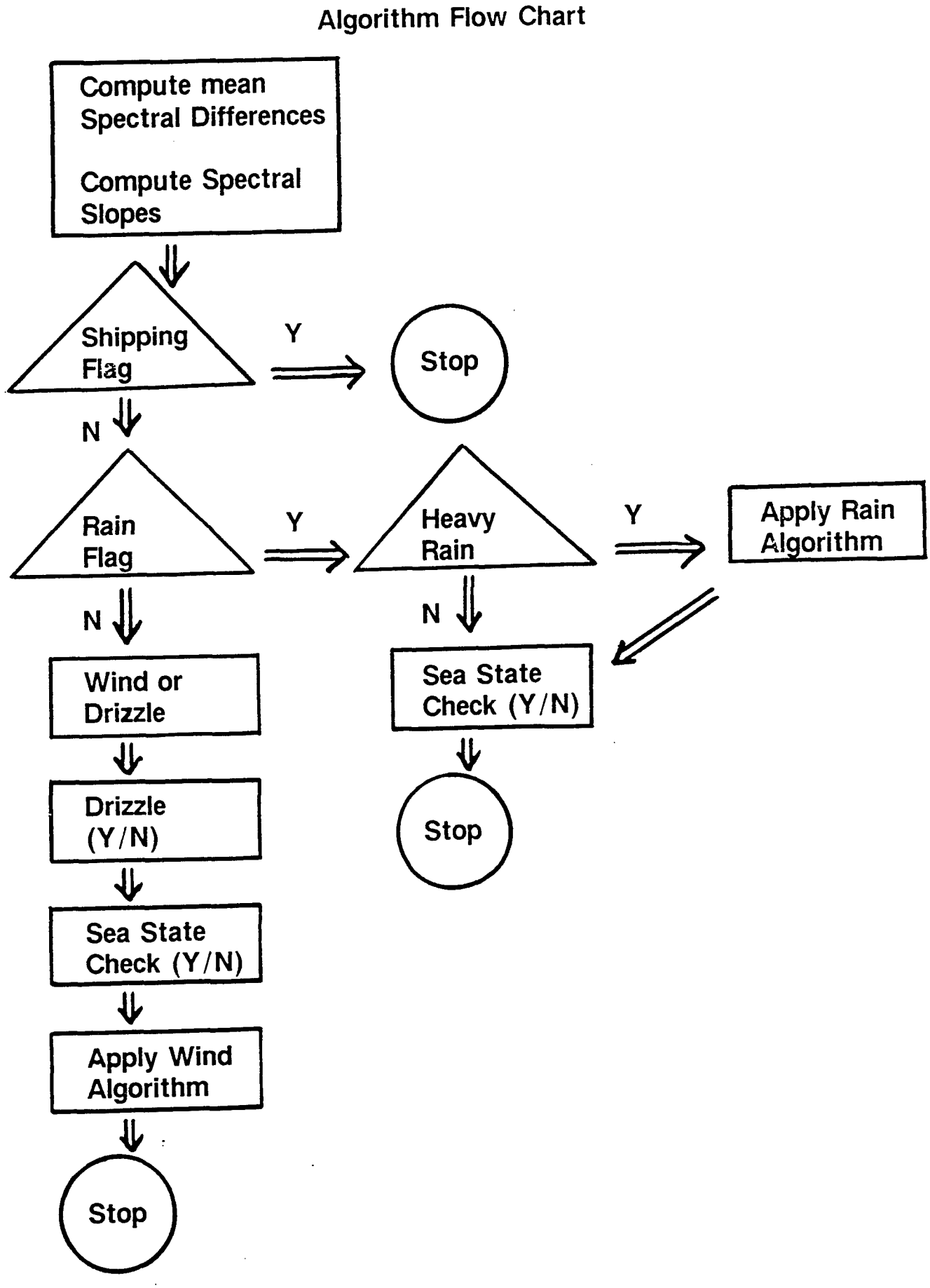

Figure 11. Flow chart for identification of the sound source based on spectral shape.

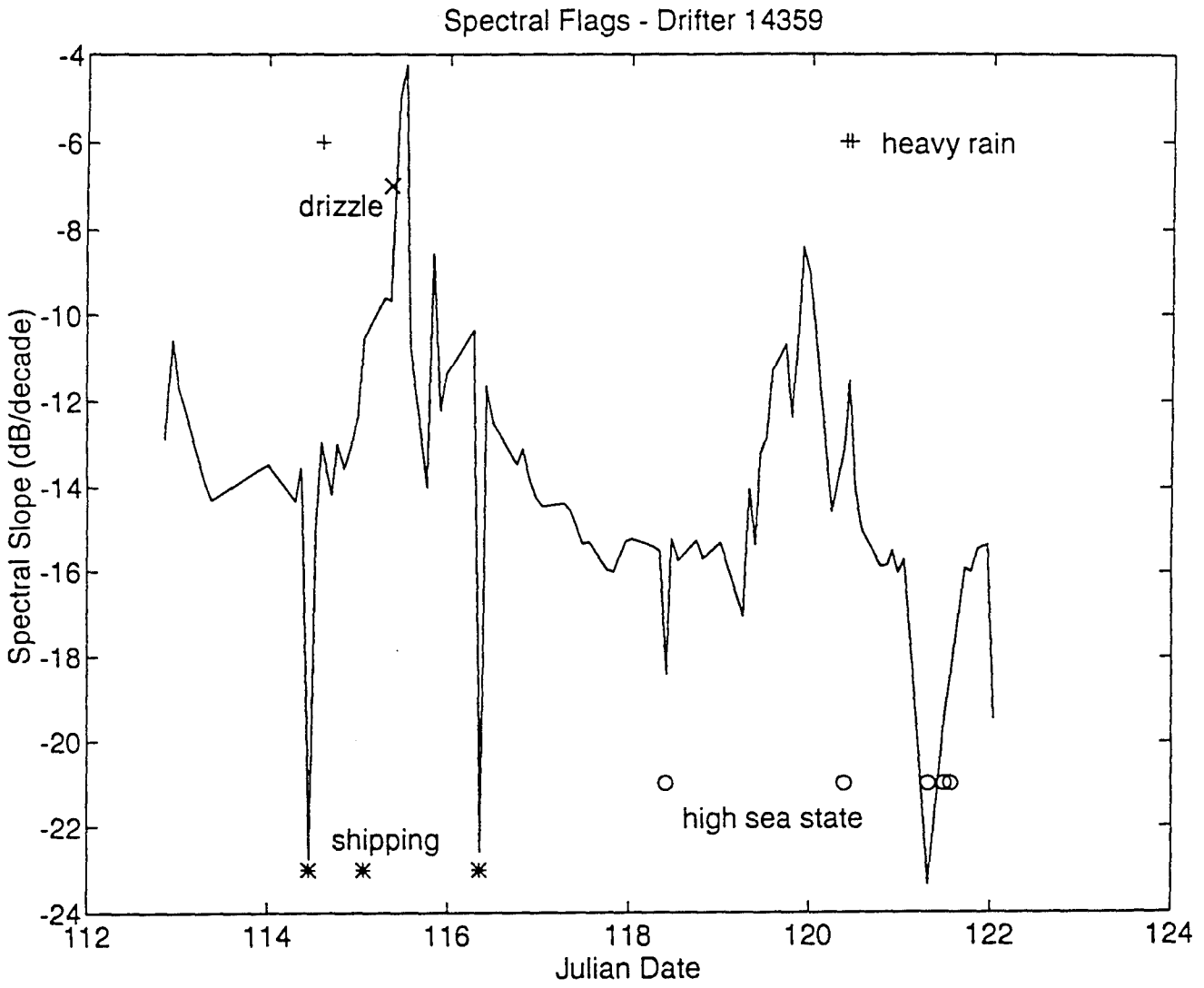

Figure 12. Mean spectral slope between 500 Hz and 25 kHz for Drifter #14359. Sound source identification using the flow chart shown in Fig. 11 (drizzle, rain, shipping and high sea state) are also indicated. The "high sea state" on JD 118 is, in fact, probably a "shipping" detection. The Vagle et al. (1990) value of -19 dB/decade for wind generated sound does not work for these data.

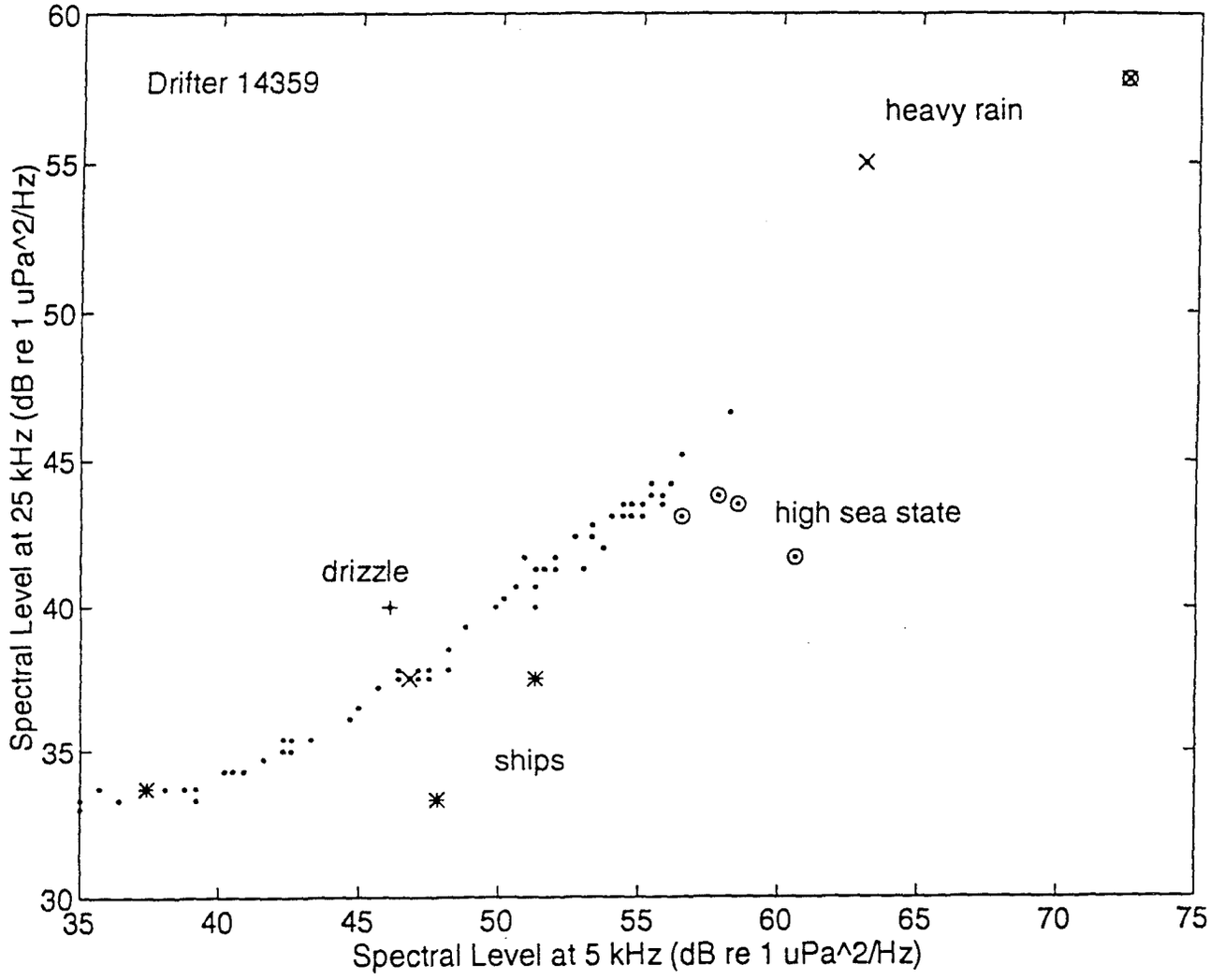

Figure 13. A comparison of sound intensity at 5 and 25 kHz for Drifter #14359. Detection of shipping (*), high sea state (o), drizzle (+), rain (x) and wind only (dots) is accomplished by clustering of points on this type of figure.

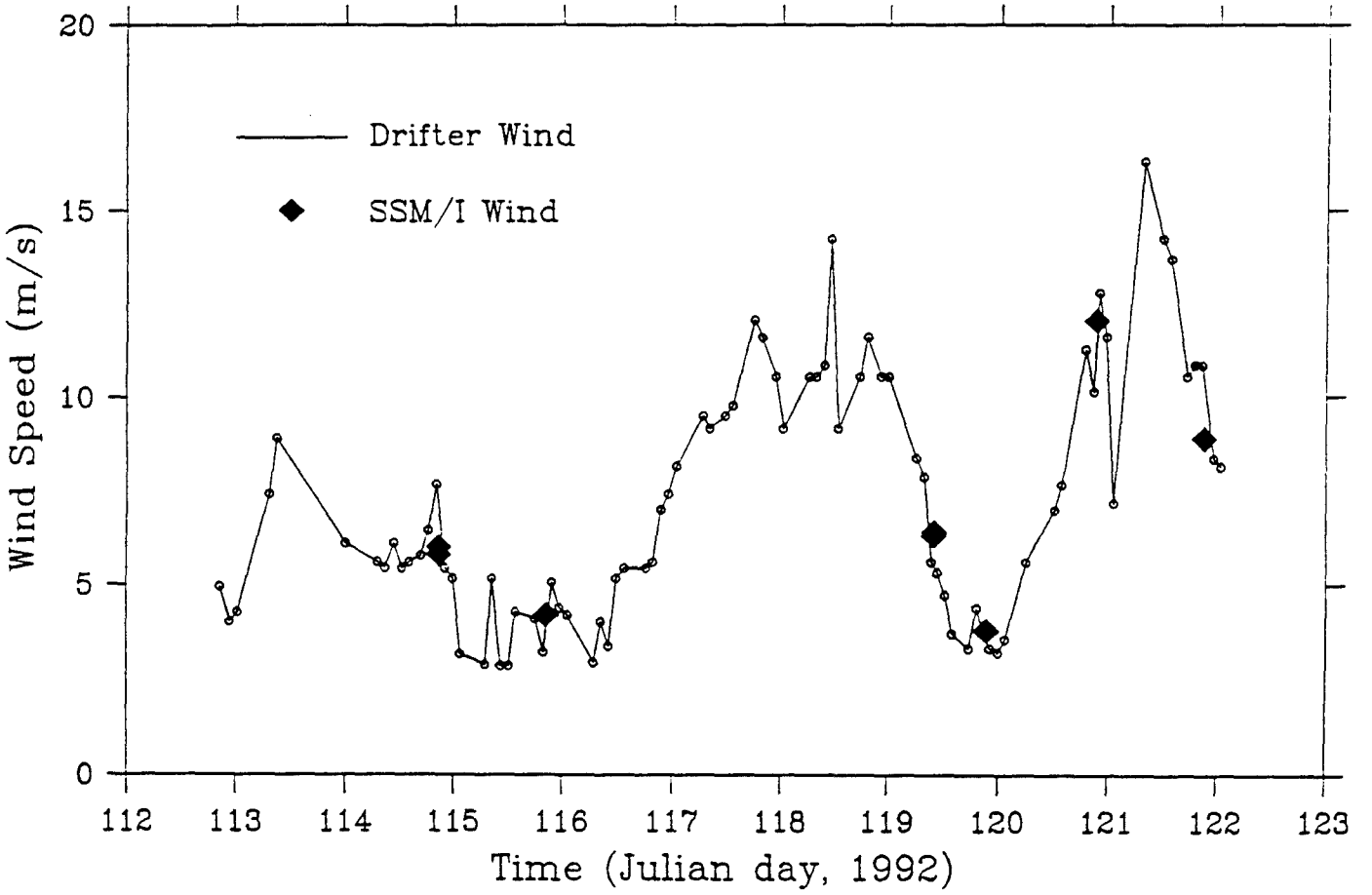

Figure 14. A comparison of acoustically derived wind speeds from Drifter #14359 and satellite derived wind speeds (SSM/I) at the drifter location.

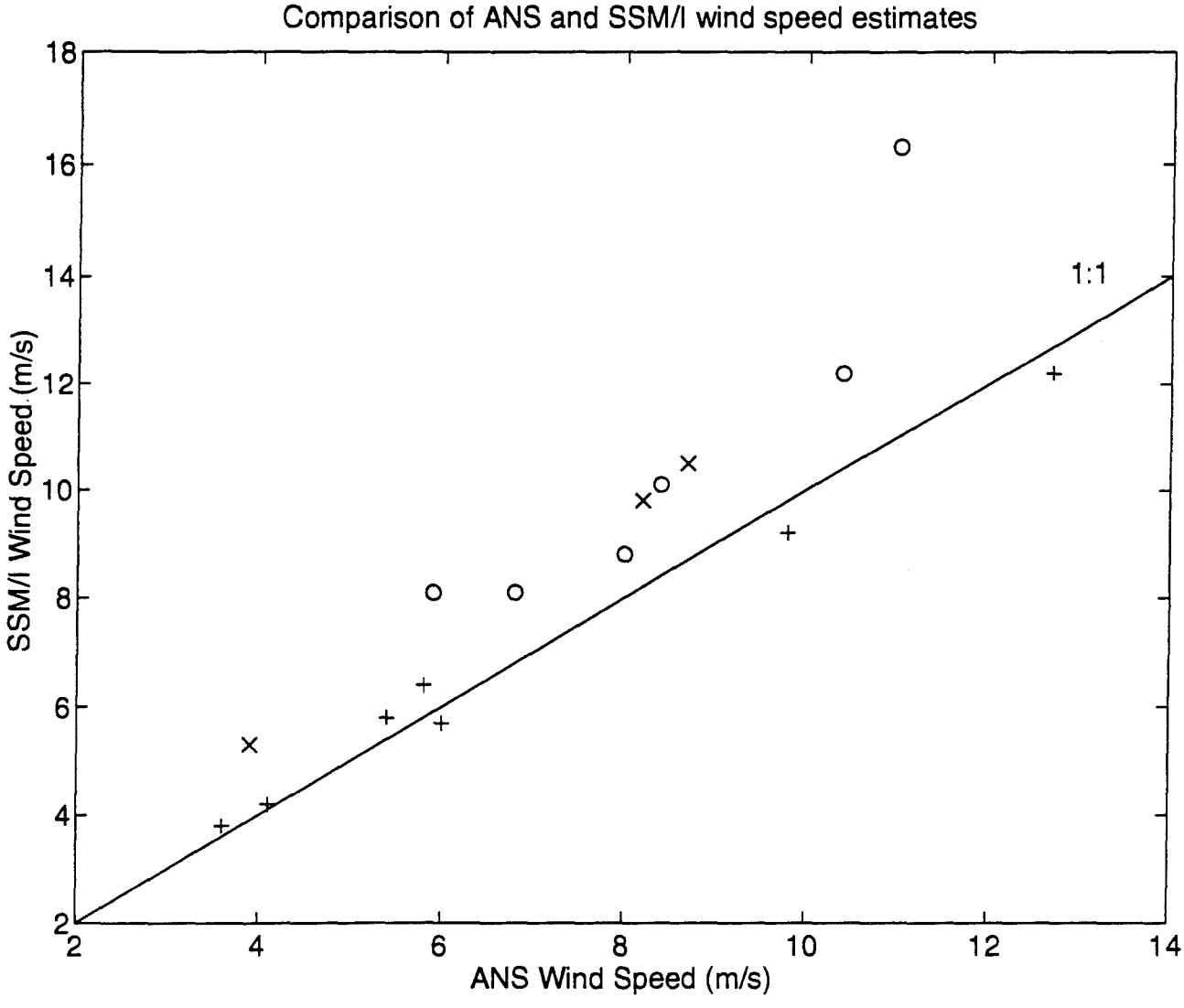

Figure 15. A comparison of acoustically derived wind speeds and satellite wind speeds for several independent deployments of acoustic drifters. The deployments were in the North Pacific, North Atlantic and Gulf of Mexico.

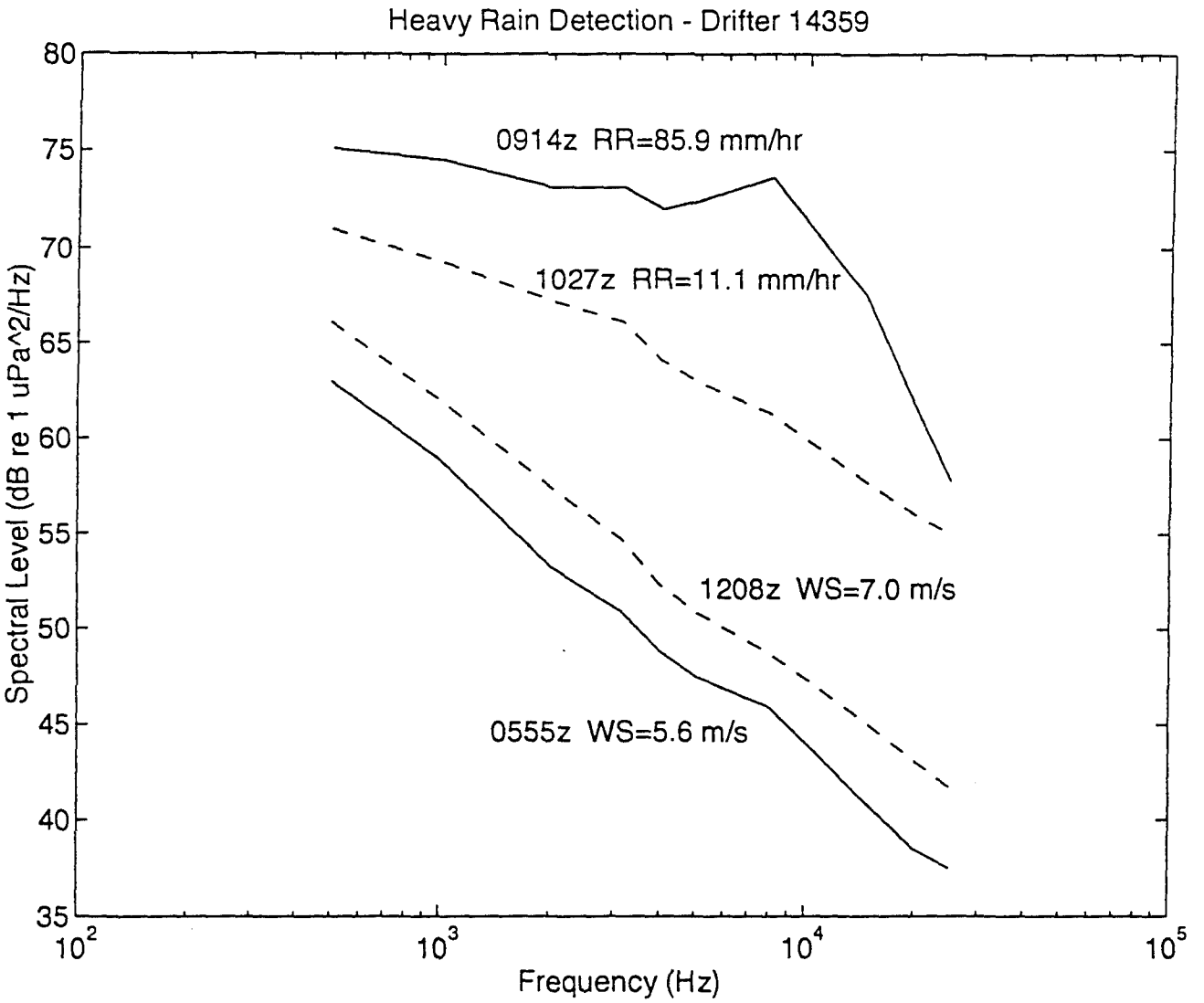

Figure 16. Acoustic detection of heavy rain from Drifter #14359. Two "wind only" spectra (at 0555z and 1208z) are also shown. The quantitative estimates of rainfall rate use the algorithm of Nystuen et al. (1993). The wind speed is estimated using the algorithm of Vagle et al. (1990).

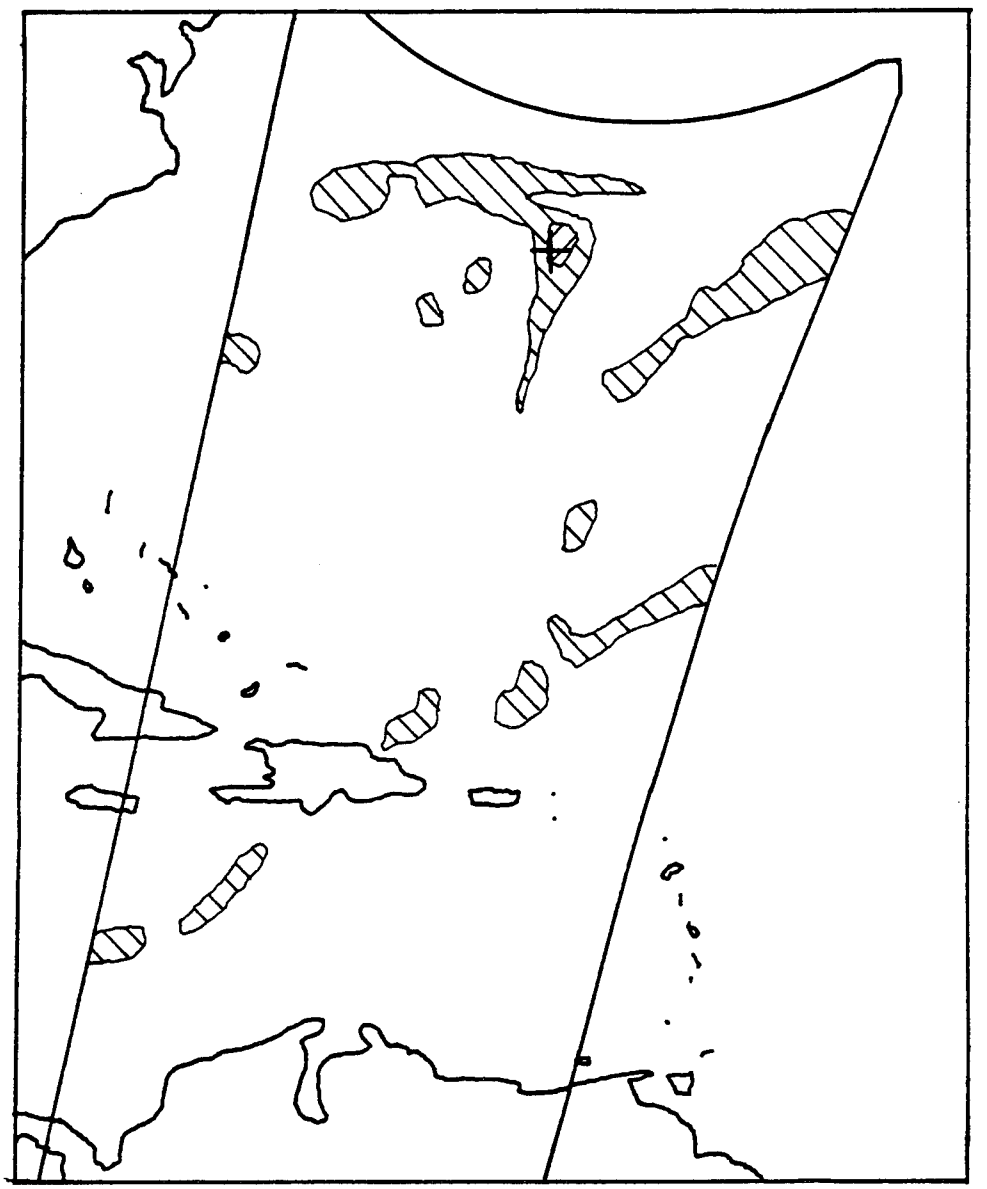

Figure 17. The microwave (SSM/I) satellite image for rainfall rate one minute prior (at 0913z) to the acoustic rainfall detection (at 0914z) on JD 120. The + shows the buoy location. The shaded areas show rainfall over 1 mm/hr. At the buoy location the rainfall rate is over 5 mm/hr.

REPORT DOCUMENTATION PAGE

Form Approved
OBM No. 0704-0188

1. AGENCY USE ONLY *(Leave blank)*	2. REPORT DATE	3. REPORT TYPE AND DATES COVERED
	June 1995	Contract Report

4. TITLE AND SUBTITLE

Monitoring Air/Sea Interaction Processes Using Passive Acoustic Drifters (AN/WSQ-6 Buoys)

5. FUNDING NUMBERS

Job Order No. 74-5138-00
Program Element No. 0604218N
Project No.
Task No. R-17400S
Accession No. DN153-136

6. AUTHOR(S)

Jeffrey a. Nystuen*

7. PERFORMING ORGANIZATION NAME(S) AND ADDRESS(ES)

Cooperative Institute for Marine and Atmospheric Studies
Rosenstiel School for Marine and Atmospheric Sciences
University of Miami
Miami, Florida

8. PERFORMING ORGANIZATION REPORT NUMBER

NRL/CR/7410--95-0051

9. SPONSORING/MONITORING AGENCY NAME(S) AND ADDRESS(ES)

Chief of Naval Research
Arlington, VA 22217

10. SPONSORING/MONITORING AGENCY REPORT NUMBER

11. SUPPLEMENTARY NOTES

12a. DISTRIBUTION/AVAILABILITY STATEMENT

Approved for public release; distribution is unlimited.

12b. DISTRIBUTION CODE

13. ABSTRACT *(Maximum 200 words)*

An acoustic min-drifting buoy designed to meet operational naval demands for real time monitoring of upper ocean air/sea interface processes is described. The AN/WSQ-6 (XAN-2) acoustic drifting buoy is an air-deployable, standard sonobuoy-sized buoy. When deployed, a hydrophone suspended below a small surface float. Data collected by the system are transmitted to users via ARGOS satellite link. Atmospheric pressure, air and sea temperature, and ambient sound levels are measured directly. Indirect measurements of wind speed and precipitation are made using the ambient sound field data.

14. SUBJECT TERMS

buoys, atmospheric pressure, sea temperature

15. NUMBER OF PAGES

30

16. PRICE CODE

17. SECURITY CLASSIFICATION OF REPORT	18. SECURITY CLASSIFICATION OF THIS PAGE	19. SECURITY CLASSIFICATION OF ABSTRACT	20. LIMITATION OF ABSTRACT
Unclassified	Unclassified	Unclassified	SAR